

FTIR and UV Spectroscopy of Parallel-Stranded DNAs with Mixed A•T/G•C Sequences and Their A•T/I•C Analogues

Shahla Mohammadi,[‡] Reinhard Klement,[§] Anna K. Shchvolkina,^{||} Jean Liquier,[‡] Thomas M. Jovin,[§] and Eliane Taillandier^{*,‡}

URA CNRS 1430, University of Paris XIII, F-93017 Bobigny, France, Engelhardt Institute of Molecular Biology, Russian Academy of Science, 117984 Moscow, Russia, and Department of Molecular Biology, Max Planck Institute for Biophysical Chemistry, D-37077 Göttingen, Germany

Received May 15, 1998; Revised Manuscript Received September 21, 1998

ABSTRACT: The infrared spectra of parallel-stranded (ps) hairpin duplexes with mixed A•T/G•C composition and either isolated or sequential G•C pairs were studied in comparison with antiparallel-stranded (aps) duplexes and a corresponding set of molecules with hypoxanthine as a G base analogue lacking the exocyclic amino group. The ps duplexes showed the characteristic bands for the C2=O2 and C4=O4 stretching vibrations of thymine residues in *trans*-Watson–Crick A•T pairing at 1683 and 1668 cm⁻¹. The latter band was superimposed on the stretching vibration of the free C6=O6 group of guanine. Substitution of guanine by hypoxanthine inhibited the formation of ps hairpin duplexes whatever the sequence, demonstrating that in the H-bonding between G and C the 2-NH₂ group is necessary for stabilizing all of the investigated ps duplexes. This result is in agreement with a model of *trans*-Watson–Crick G•C base pairs with two H-bonds [N2H₂(G)–N3(C) and N1H(G)–O2(C)]. However, *trans*-Watson–Crick A•T and G•C base pairs with two H-bonds are not isomorphous, which may explain the decreased stability of the ps, but not the aps, duplexes upon increasing the number of A•T/G•C steps. Molecular modeling studies performed on two of the ps duplexes reveal the existence of propeller twist for avoiding a clash between the N2(G) and N4(C) amino groups, and favorable stacking of sequential G•C base pairs. The optimized hairpin ps duplexes invariably incorporated G•C base pairs with two H-bonds, regardless of the initial structures adopted for the force field calculations.

Classical right-handed double-stranded DNAs and RNAs belonging to the B and A families are formed by two antiparallel strands hybridized via A•T and G•C Watson–Crick base pairs. The latter are isomorphous, leading to very regular double-helical structures. Experimental data have confirmed the feasibility of reversing the sense of the double helix from right-handed to left-handed while maintaining Watson–Crick base pairing (1, 2). More recently, it has been demonstrated that one can also invert the relative orientation of the two strands, thereby obtaining parallel-stranded (ps) double-stranded DNA (3–6). Ps duplexes containing only A•T base pairs or incorporating few G•C base pairs have been studied by Raman spectroscopy (7) and FTIR¹ (8) to elucidate the base pairing configurations. Both methods have shown that A•T base pairs are of the *trans*-Watson–Crick H-bonded type, in agreement with the theoretical model proposed initially for ps-DNA duplexes by Pattabiraman (9). However, the low GC content of such molecules (<12%) did not permit conclusions regarding the

nature of the G•C base pairs. Two theoretical models have been proposed for *trans*-Watson–Crick G•C base pairing, featuring either one or two H-bonds between G and C (10, 11); the base pairs with two H-bonds are not isomorphous (Figure 1, models b and f). Recent energy minimization calculations suggest that the energy differences between ps and aps duplex models based exclusively on G•C base pairs arise mainly from base stacking (11). Furthermore, ps duplexes featuring one H-bond between G and C are presumed to be less stable than those with two H-bonds (12).

Experimental demonstrations of ps duplexes incorporating both A•T and G•C (up to 40%) base pairs have been reported (13, 14). More recently, thermodynamic studies of ps hairpin duplexes have shown important differences in stability correlated with the distribution of the G•C base pairs within AT tracts (A.K.S. and T.M.J., unpublished data). The manner in which the G bases are distributed within the sequence (consecutive or scattered) is reflected in the number of steps between G•C and A•T base pairs, and thus the magnitude of the potential destabilizing effects exerted by these steps. We have investigated by FTIR spectroscopy and UV thermal denaturation a series of oligomers comprising two decameric sequences connected 5'–5' via nonnucleotide linkers, and thereby constrained to fold back into ps hairpins. The sequences were designed with variable numbers of A•T/G•C steps so as to permit an assessment of their influence on the formation and stability of the ps

* Correspondence should be addressed to this author at URA CNRS 1430, Université Paris XIII, 74 Rue Marcel Cachin, F-93017 Bobigny, France.

[‡] University of Paris XIII.

[§] Department of Molecular Biology, Max Planck Institute for Biophysical Chemistry.

^{||} Engelhardt Institute of Molecular Biology.

¹ Abbreviations: H-bond(ing), hydrogen bond(ing); FTIR, Fourier transform infrared.

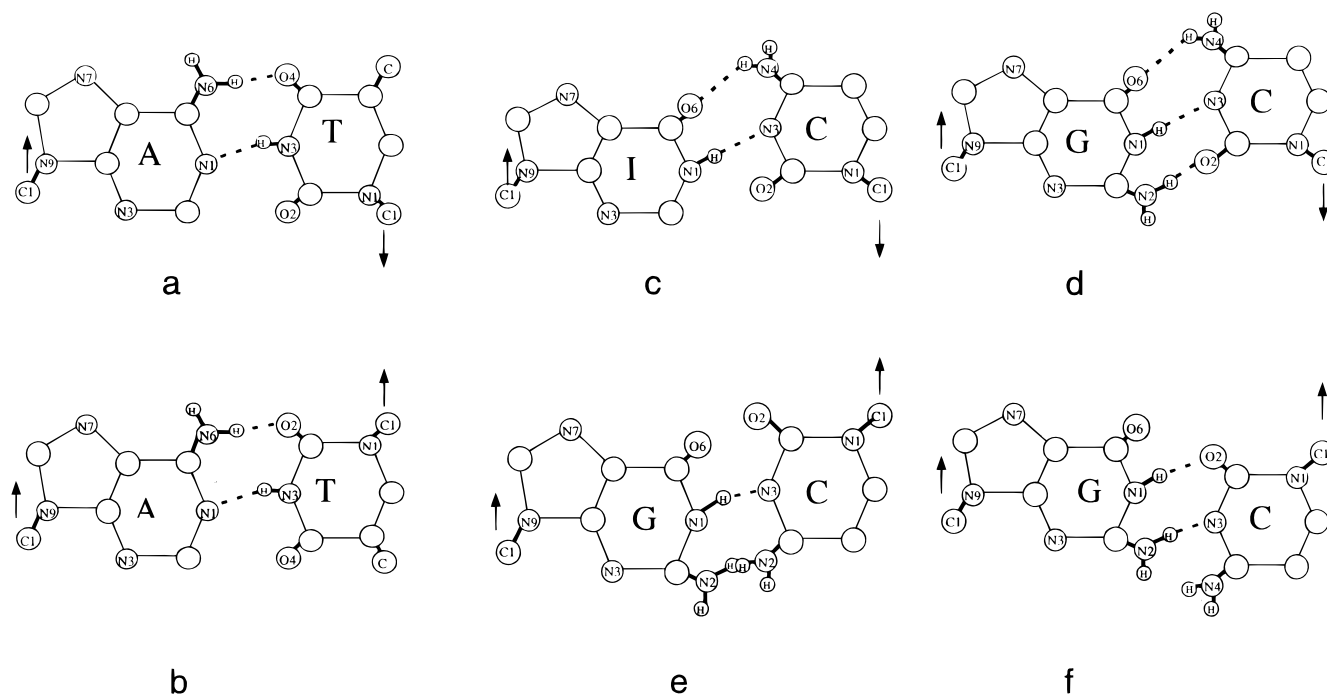


FIGURE 1: Models for base pairing in *cis*-Watson-Crick and *trans*-Watson-Crick conformation. Reproduced with permission from ref (11). (a) *cis*-Watson-Crick A•T pair, as observed in a canonical antiparallel DNA double-helix, with two H-bonds between N1H(A)–O4(T) and N6H₂(A)–O4(T). (b) *trans*-Watson-Crick A•T pair with two H-bonds between N1H(A)–N3H(T) and N6H₂(A)–O2(T) instead of O4(T) in *cis*-Watson-Crick A•T. (c) *cis*-Watson-Crick I•C pair with two H-bonds between N1H(I)–N3(C) and O6(I)–N4H₂(C). (d) *cis*-Watson-Crick G•C pair with three H-bonds between N1H(G)–N3(C), N2H₂(G)–O2(C), and O6(G)–N4H₂(C) as observed in a canonical antiparallel DNA double-helix. (e) *trans*-Watson-Crick G•C pair with a single H-bond between N1H(G)–N3(C). (f) *trans*-Watson-Crick G•C pair with two H-bonds between N1H(G)–O2(C) and N2H₂(G)–N3(C).

duplexes. Control experiments were performed on oligomers with the same sequences in the conventional aps orientation.

In the *trans*-Watson-Crick G•C base pair model with one H-bond (Figure 1e), sites N1H(G) and N3(C) are linked, whereas in the model with two H-bonds (Figure 1f) the connected sites are N1H(G)–O2(C) and N2H₂(G)–N3(C). Hypoxanthine is a guanine analogue lacking the exocyclic amino group at position 2. Therefore, to determine the involvement of the amino group in the H-bonding pattern, i.e., to distinguish between the alternative secondary structures, we used oligonucleotides in which the guanines were substituted by hypoxanthine. In addition to the systematically lower stability of the ps duplexes compared to the corresponding aps references, substitution of guanine by hypoxanthine has a destabilizing effect in the case of both the ps and aps duplexes. In fact, the ps structures do not form at all. The FTIR and UV data are consistent with the presence of *trans*-Watson-Crick A•T and G•C base pairs with two H-bonds in all the ps duplexes formed. A molecular modeling calculation was performed on two of the molecules containing a low or high number of A•T/G•C steps. The energetically most favorable structures in both cases contained exclusively G•C base pairs with two H-bonds, in agreement with the experimental data.

MATERIALS AND METHODS

Materials. The oligonucleotides studied by FTIR were as follows: ps-N1, 3'-d(CTATAGGGAT)-L-d(ATCCCTATAG)-3'; ps-N2, 3'-d(CTGAGTAGAT)-L-d(ATCTACTCAG)-3'; ps-N3, 3'-d(CGTATAGGAT)-L-d(ATCCTATACG)-3'; ps-N6, 3'-d(TTATAGGGAT)-L-d(ATCCCTATAA)-3'; ps-N7, 3'-d(TTGAGTAGAT)-L-d(ATCTACTCAA)-3'; ps-N8,

3'-d(TTATAIIAT)-L-d(ATCCCTATAA)-3'; ps-N9, 3'-d(TIAITAIAT)-L-d(ATCTACTCAA)-3'; aps-N2, 5'-d(CTGAGTAGAT)-L-d(ATCTACTCAG)-3'; aps-N6, 5'-d(AATATCCCTA)-L-d(TAGGGATATT)-3'; aps-N7, 5'-d(AACTCATCTA)-L-d(TAGATGAGTT)-3'; aps-N8, 5'-d(AATATCCCTA)-L-d(TAIIATATT)-3'; aps-N9, 5'-d(AAATCATCTA)-L-d(TAIIATATT)-3'; in which L represents the linker -PO(CH₂CH₂O)₃P-.

Ps-N1, ps-N3, and aps-N2 were purchased from Genset. Ps-N2 was synthesized by the Bioengineering Center of the Russian Academy of Science. The other oligonucleotides were synthesized by BioTez Berlin-Buch GmbH. To remove excess salt, all these oligonucleotides were purified and desalted using an Ultra-Mc filter (Millipore).

UV-Visible Spectroscopy. Oligonucleotide concentrations were determined from A₂₆₀ at pH 7 and 80 °C, measured with a Kontron Uvikon 942 spectrophotometer. For denaturation experiments, oligonucleotides were dissolved to a 2 μM strand concentration in 10 mM sodium-cacodylate buffer, pH 7, 100 mM LiCl. The temperature of the cell holder was varied (0.15 °C/min) by a circulating Huber water bath controlled by a PD415 temperature programmer. Melting temperatures (T_m) were determined from the first derivative of the melting curves. We use the term "duplex" in reference to paired intramolecular hairpin conformations of the oligonucleotides.

Vibrational Spectroscopy. FTIR spectra were recorded using a Perkin-Elmer 2000 spectrophotometer. The temperature of the samples was controlled and monitored between 2 and 85 °C using a Specac temperature controller; 15 scans were usually accumulated. FTIR spectra were analyzed with the Galaxy Grams 386 program. The data

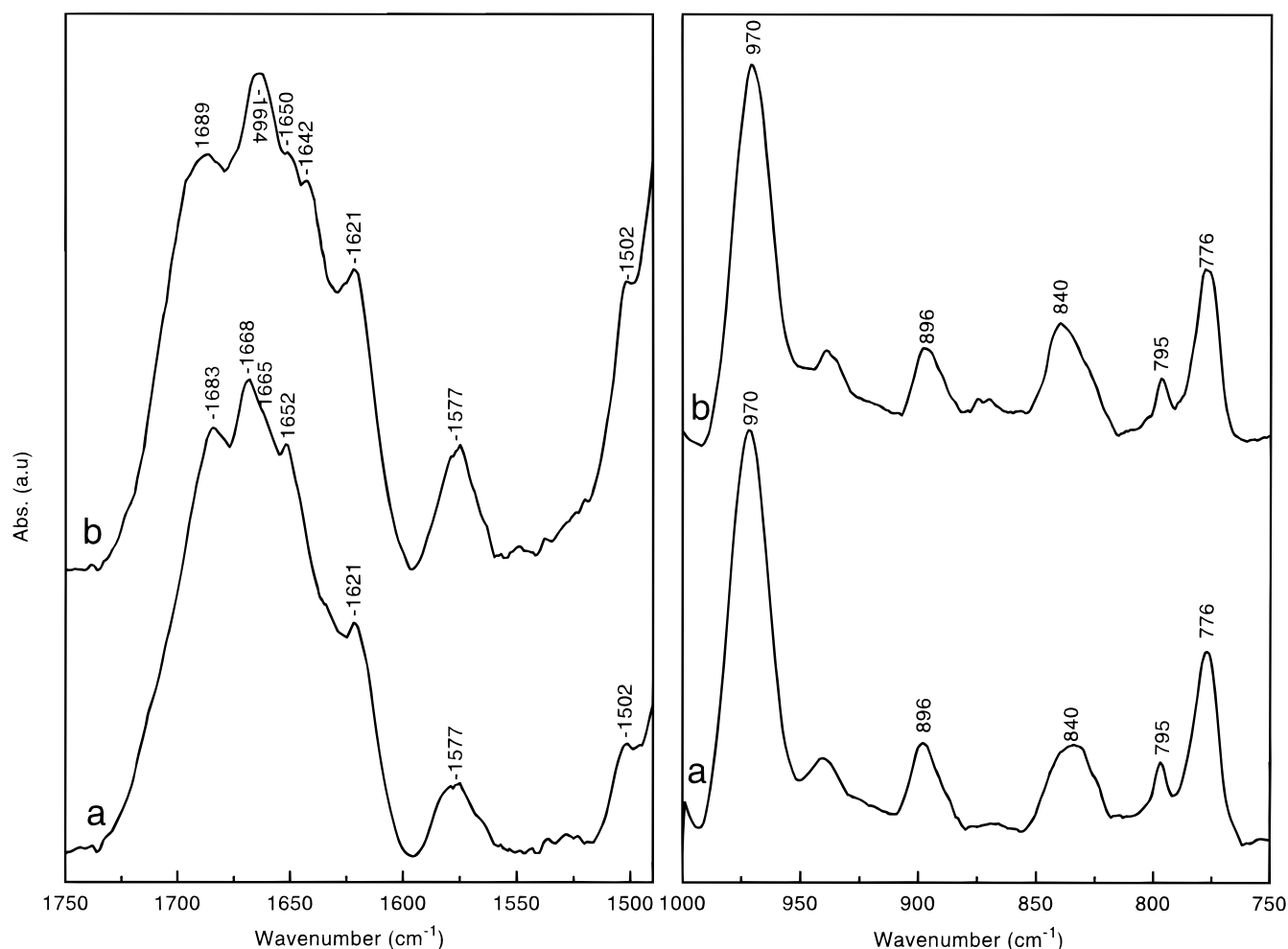


FIGURE 2: FTIR spectra, recorded in D_2O solution at 5 °C, of (a) ps-N6 in the presence of 2 Li^+ /nucleotide; and (b) aps-N6 in the presence of 1 added Li^+ /nucleotide. Left panel: domain containing absorptions of in-plane base double-bond stretching vibrations. Right panel: domain containing absorptions characteristic of sugar conformations.

treatment included multiple point base line correction and spectral normalization using the integration of the phosphate symmetric stretching vibration at 1086 cm^{-1} as an internal standard. To obtain the intramolecular duplexes, the stock solutions at pH 7 (measured with a MI4152 microcombination probe from Microelectrode Inc.) were annealed at 80 °C for 10 min and then cooled immediately to 4 °C. The oligonucleotides were studied in the presence of LiCl (1–2 Li^+ added per nucleotide) at a strand concentration of 9 mM. The sample solutions were deposited (in the cold room, 4 °C) between ZnSe windows. Deuteration experiments were performed by drying the samples under nitrogen, at 4 °C and redissolving in D_2O .

Force Field Calculations. Models of the ps-N1 and ps-N2 structures without the linker were generated using the NAMOT program (15). For both sequences, model variants were considered in which the G•C base pairs had either one or two H-bonds at the outset of the minimization procedure performed with AMBER 5.0 (16). For each variant, we generated start structures with a combination of 5 different initial values for the average twist and 5 different initial values for the average rise, giving rise to a total of 25 different structures. A total of 100 different structures were minimized. A distance-dependent dielectric constant of 4 and a nonbonded cutoff distance of 25 Å were used. All structures were minimized until the rms value of the energy

gradient was <0.05 . The color images were generated with the SCHAKAL92 program of E. Keller (University of Freiburg, Germany).

RESULTS AND DISCUSSION

Comparison of the IR Spectra of Ps-DNA and Aps-DNA. Figure 2 (left panel) shows the FTIR spectra of ps-N6 and aps-N6 (spectra a and b, respectively) in the region of the in-plane double-bond stretching vibrations of the bases. The spectra were recorded at 5 °C to favor the formation of hairpin duplexes. Striking differences were found in the carbonyl stretching vibrations of the thymine and guanine residues depending on the relative orientations of the DNA strands. The absorption bands of the ps-N6-DNA spectrum were assigned by comparison with aps-N6-DNA and with the spectra of ps-DNAs with sequences containing only A and T (8).

The aps-N6 spectrum (Figure 2b) exhibited the well-known carbonyl stretching bands of classical *cis*-Watson–Crick base pairs (17). The $C4=O4$ stretching vibration of thymine was located at 1664 cm^{-1} while those of the $C2=O2$ group of the same residues and of the $C6=O6$ of the guanine residues were superimposed at 1689 cm^{-1} (Figure 2b).

In the ps-N6-DNA spectrum, the broad band at 1689 cm^{-1} disappeared, being replaced by a new band at 1683 cm^{-1}

Table 1: FTIR Bands Observed at 5 °C between 1750 and 1550 cm⁻¹

		FTIR bands (cm ⁻¹)				
		Oligonucleotides				
ps-N1		1683	1668	1652		1621
ps-N2		1683	1668	1652	1642(sh) ^a	1621
ps-N3		1683	1668	1652		1621
ps-N6		1683	1668, 1665(sh)	1652		1621
ps-N7	1689			1664	1650	1629
aps-N2	1689			1673	1650	1642
aps-N6	1689			1664	1650	1642
		Hypoxanthine Analogues				
ps-N8	1689			1664	1653	1629
ps-N9	1689			1664		1627
aps-N8	1689			1664	1653	1642
						1621

^a sh, shoulder.

and a broad band with a shoulder at 1668 cm⁻¹ (Figure 2a). In a previous study of ps duplexes containing only A•T base pairs, both the C2=O2 and C4=O4 stretching modes of thymine showed strong absorption bands located at 1685 and 1668 cm⁻¹, respectively (8). Accordingly, both the 1683 and 1668 cm⁻¹ absorption bands of ps-N6-DNA are assigned to C2=O2 and C4=O4 stretching vibrations of thymine, respectively. We also conclude that the C6=O6 carbonyl stretching band of guanine was downshifted and possibly superimposed on the C4=O4 stretching vibration of thymine at 1668 cm⁻¹. A similar spectral behavior of the C=O groups of the thymine and guanine residues was observed for all the ps-DNAs studied here having four bases, with the exception of ps-N7-DNA (Table 1).

In relation to the two carbonyl stretching vibrations of thymine, it has been proposed previously for ps-DNA with only A and T bases that frequency shifts reflect the reversed engagement of C2=O2 and C4=O4 groups in the *trans*-Watson–Crick base pair compared to the canonical *cis*-Watson–Crick A•T base pair. The similar shifts observed for the carbonyl groups of thymine in ps-DNA having all four bases constitute evidence for the preservation of the same A•T pairing configuration, i.e., with thymine H-bonded at position 2.

The formation of the second H-bond in the A•T base pair was evidenced by the presence of an absorption at 1281 cm⁻¹ in the spectra of ps-N1 and ps-N6 recorded in H₂O (not shown). This absorption was observed at the same position in the aps duplexes, and reflects a stretching vibration of the thymine involving the CN3H group (18). Upon thermal denaturation of ps-N1 and ps-N6, the band was shifted to lower wavenumbers and the relative intensity increased, indicating the breakage of the N3H(T)–N1(A) H-bond.

A low-frequency shift of the carbonyl frequency of the guanine residues was observed upon passing from aps-N6-DNA to ps-N6-DNA. In agreement with both models proposed for G•C *trans*-Watson–Crick base pairs (Figure 1e,f; 10, 11, 19), the C6=O6 group of the guanine appears not to be involved in the H-bonding between G and C. Therefore, the ps hairpins are expected to have free C6=O6 groups, giving rise to an absorption around 1668 cm⁻¹ [the position of the dGMP band in dilute solution, (17)]. The observed frequency for all ps-DNAs, except ps-N7-DNA, was 1668 cm⁻¹ (Table 1). Thus, the position of the C6=O6 stretching vibration of the guanine residues in ps-DNAs with mixed sequences is in agreement with the formation of

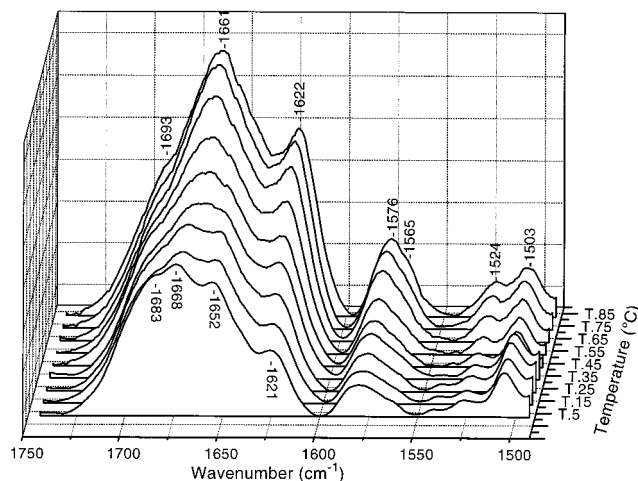


FIGURE 3: FTIR spectra of ps-N1 in the domain containing absorptions of in-plane base double-bond stretching vibrations, recorded in D₂O solution in the presence of 2 added Li⁺/nucleotide, at 5–85 °C.

trans-Watson–Crick G•C pairs. However, it should be noticed that unpaired G bases would also have free carbonyl groups.

The ps hairpins had sequences containing either consecutive guanines (ps-N1-DNA, ps-N3-DNA, ps-N6-DNA) or separated guanines with a terminal G (ps-N2-DNA). A different behavior was seen for the sequence containing separated guanines but without a terminal G (ps-N7-DNA). As mentioned above, the ps-N7 hairpin duplex was not stable under the conditions used for FTIR spectroscopy. The characteristic absorptions of *trans*-Watson–Crick thymines at 1683 cm⁻¹ and of *trans*-Watson–Crick guanines at 1668 cm⁻¹ were not observed in the spectra of ps-N7-DNA (Table 1). Instead, an absorption at 1689 cm⁻¹ appeared.

With respect to the sugar backbone conformation, we note that changing the strand orientation from aps to ps did not alter the sugar pucker (Figure 2, right panel). That is, the spectra of ps-N6 and aps-N6 displayed the same absorption located around 840 cm⁻¹, characteristic of the C2'-endo sugar pucker (20). Moreover, the presence of an absorption at 1375 cm⁻¹ in the spectrum of ps-N6, i.e., at the same position as for aps-N6 (data not shown), indicated that the base–sugar orientation remained anti upon reversal of the strand orientation.

Thermal Denaturation. To provide more information on the stability and base pairing patterns of ps-DNA, we carried

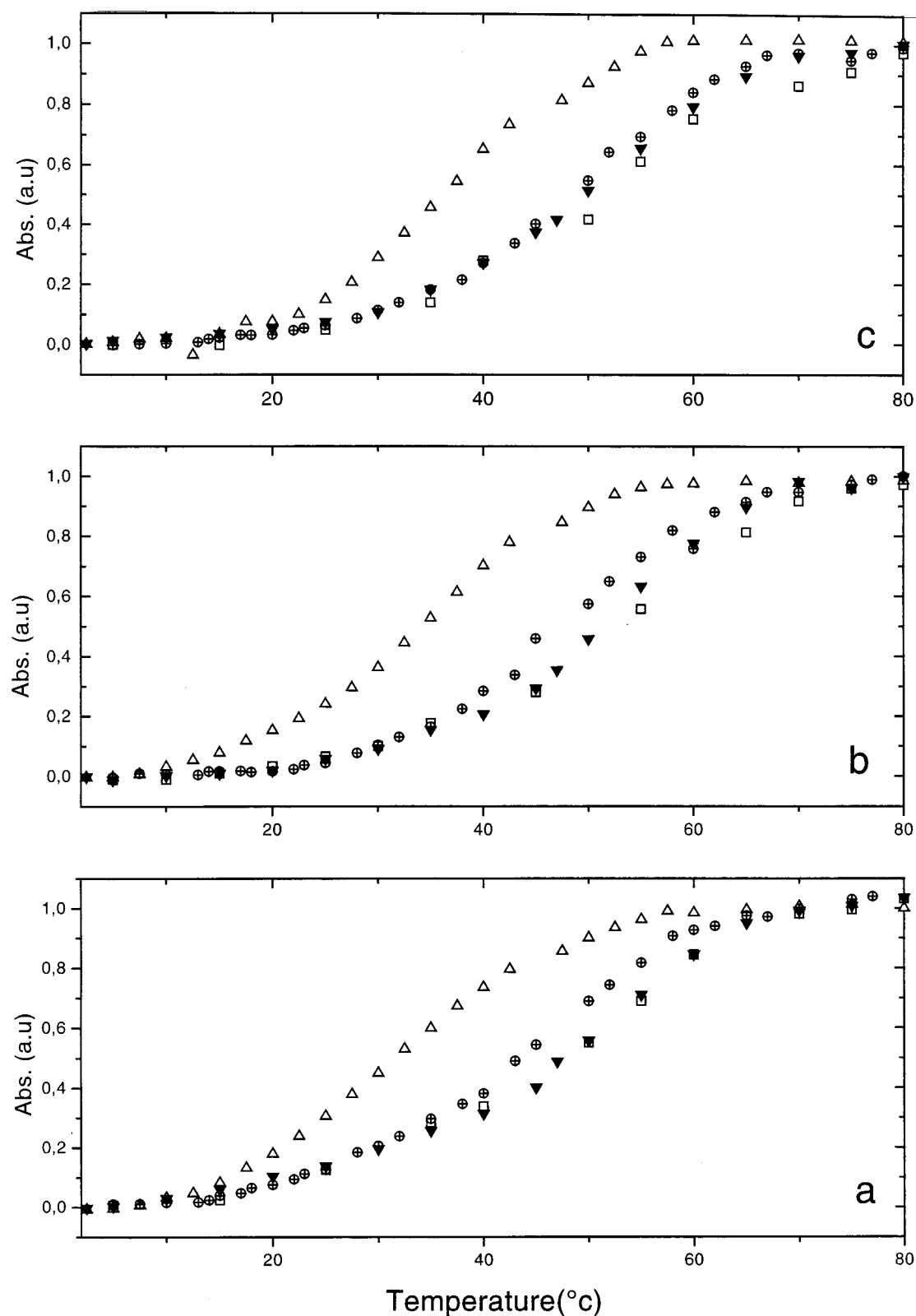


FIGURE 4: Normalized intensities of the FTIR bands versus temperature. (\square) ps-N1; (Δ) ps-N2; (\oplus) ps-N3; (\blacktriangledown) ps-N6. (a) Adenine band at 1621 cm^{-1} . (b) Guanine band at 1576 cm^{-1} . (c) Cytosine band at 1524 cm^{-1} .

out thermal denaturation experiments. The significant intensity changes and frequency shifts induced by temperature increase in the range $5\text{--}85\text{ }^{\circ}\text{C}$ are given in Figure 3 for the spectra of ps-N1-DNA. The shift of the C2=O2 stretching mode of thymine from 1683 to 1693 cm^{-1} upon thermal denaturation confirmed the participation of the keto group in H-bonding. After melting, the wavenumber of this

band was the same as that observed for unpaired thymines of single-stranded oligomers (20). The other carbonyl stretching modes (C4=O4 of thymine, C6=O6 of guanine, and C2=O2 of cytosine) were superimposed at 1661 cm^{-1} , and thus did not serve to characterize modifications in the interactions between the bases upon thermal denaturation. Instead, the marked increases in the intensities of three

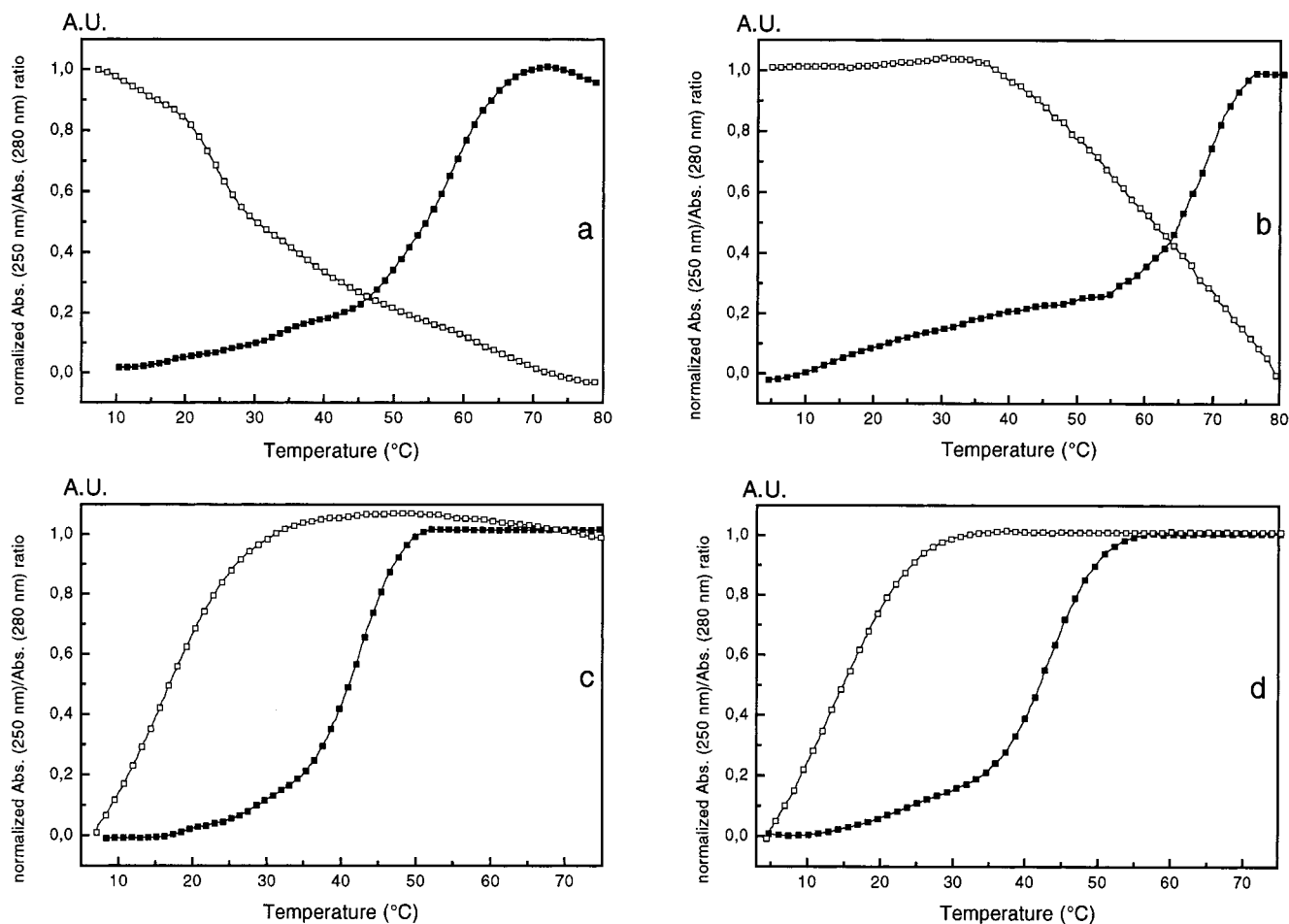


FIGURE 5: Normalized ratio of UV absorbances at 250 and 280 nm versus temperature. (a) (□) ps-N6, (■) aps-N6; (b) (□) ps-N7, (■) aps-N7; (c) (□) ps-N8, (■) aps-N8; (d) (□) ps-N9, (■) aps-N9.

$$A_{250/280}^{\text{norm}} \equiv ([A_{250}/A_{280}]^T - [A_{250}/A_{280}]^{T_{\min}})/([A_{250}/A_{280}]^{T_{\max}} - [A_{250}/A_{280}]^{T_{\min}}).$$

vibrational modes involving motions of nitrogen atoms of the six-membered rings of A, G, and C were used.

In the spectral range between 1750 and 1500 cm^{-1} , the adenine residues gave only one band at 1621 cm^{-1} (Figure 3). This mode, assigned to ND_2 scissoring coupled to ring $\text{C}=\text{C}$ and $\text{C}=\text{N}$ stretching vibrations, has been used previously to follow the melting of DNA duplexes and triplexes (21, 22). In addition to the $\text{C}6=\text{O}6$ stretching band, the guanine residues have a band at 1576 cm^{-1} assigned to $\text{C}=\text{N}$ (except $\text{C}8=\text{N}7$) and $\text{C}-\text{N}$ bond stretching vibrations (23, 24). We also used these bands to monitor the thermal denaturation of ps- and aps-DNAs. The most sensitive mode to ^{15}N isotopic substitution of cytosine was located at 1524 cm^{-1} (17), and provided local information regarding the ps-DNA and aps-DNA melting transitions (Figure 3).

The plots of the intensity variation measured at the different wavenumbers versus temperature for ps-DNA showed similar thermal profiles for the adenine, guanine, and cytosine residues belonging to the same oligonucleotide, but indicated a lower stability for ps-N2-DNA with isolated guanines than for ps-N1, ps-N3, and ps-N6-DNA (Figure 4).

The melting temperatures (T_m) evaluated from the derivative curves are summarized in Table 2 (top) together with those of aps-DNAs for comparison. The T_m values were similar, regardless of the nature of the bases involved in the

vibrational mode used for the intensity measurements, but depended in the case of ps-DNA (but not of aps-DNA) on the guanine distribution in the DNA sequences (Table 2, top). These data suggest strongly that G•C pairs formed in the ps duplexes at low temperature but that the steps between G•C and A•T base pairs reduced the stability of the ps hairpin duplexes. For example, keeping the same base composition but increasing the number of A•T/G•C steps from 3 in ps-N1 or ps-N3 to 7 in ps-N2 induced a 10 °C decrease in T_m . A further increase in A•T/G•C transitions, as in ps-N7 with 6 steps for three guanines, led to a still greater relative destabilization of the duplex, such that a stable secondary structure was no longer observed under the conditions used for FTIR spectroscopy. In contrast, the T_m values of aps-N6 and aps-N2 were very close. The lack of structural isomorphism of the A•T and G•C base pairs in the ps duplexes (Figure 1) might account in large part for their lowered thermal stability relative to aps-DNA, particularly in molecules with many sequence alternations.

In the first of the two models presented in Figure 1e,f for the *trans*-G•C base, only one H-bond is present and involves the N1H site of guanine. In the second case, both N1H and N2H₂ sites participate in H-bonding, but the base pair is not isomorphous with A•T. The role of the amino group in the formation of H-bonds in the G•C base pairs is examined further in the next section.

Table 2: Melting Temperatures Obtained by FTIR and UV Spectroscopy

	T_m (°C, ± 1 °C)			
	1621 cm^{-1} Ade band	1577 cm^{-1} Gua band	1524 cm^{-1} Cyt band	260 nm UV
Oligonucleotide				
ps-N1: 3'-d(CTATAGGGAT)-L-d(ATCCCTATAG)-3'	51	51	51	52
ps-N2: 3'-d(CTGAGTAGAT)-L-d(ATCTACTCAG)-3'	39	41	42	40
ps-N3: 3'-d(CGTATAGGAT)-L-d(ATCCTATACG)-3'	48	49	48	46
ps-N6: 3'-d(TTATAGGGAT)-L-d(ATCCCTATAA)-3'	49	50	48	48
ps-N7: 3'-d(TTGAGTAGAT)-L-d(ATCTACTCAA)-3'	—	—	—	28
aps-N2: 5'-d(CTGAGTAGAT)-L-d(ATCTACTCAG)-3'	69	70	69	68
aps-N6: 5'-d(AATATCCCTA)-L-d(TAGGGATATT)-3'	68	69	68	66
aps-N7: 5'-d(AACTCATCTA)-L-d(TAGATGAGTT)-3'	—	—	—	67
Hypoxanthine Analogues				
ps-N8: 3'-d(TTATAIIAT)-L-d(ATCCCTATAA)-3'	28 ^a	—	28	18
ps-N9: 3'-d(TTIAITAIAT)-L-d(ATCTACTCAA)-3'	—	—	—	15
aps-N8: 5'-d(AATATCCCTA)-L-d(TAIIATATT)-3'	47	—	47	45
aps-N9: 5'-d(AACTCATCTA)-L-d(TAIIATIAIT)-3'	—	—	—	45

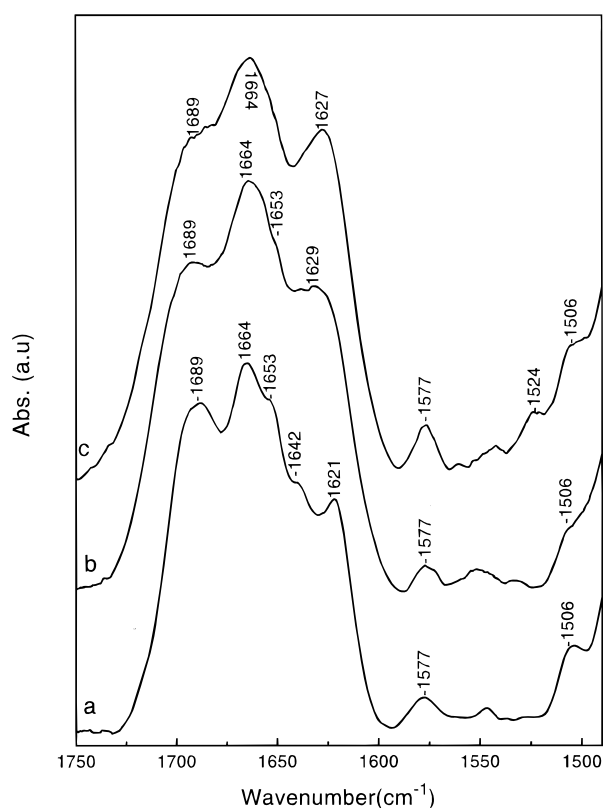
^a T_m at 1629 cm^{-1} .

FIGURE 6: FTIR spectra in the domain containing absorptions of in-plane base double-bond stretching vibrations recorded in D_2O solution at 5 °C of (a) aps-N8 in the presence of 1 added Li^+ /nucleotide, (b) ps-N8 in the presence of 2 added Li^+ /nucleotide, and (c) ps-N9 in the presence of 2 added Li^+ /nucleotide.

We performed melting experiments at low DNA concentrations by classical UV absorption. No significant differences were seen between the T_m s determined by UV or FTIR (Table 2). As predicted for the melting of intramolecular structures, the T_m s were independent of the DNA concentration. In the case of ps-N7-DNA, melting by UV was observed at 28 °C. Inasmuch as the FTIR spectra of the concentrated ps-N7 solutions failed to reveal the existence of a ps hairpin duplex, we determined whether the structure found by UV was ps or aps. It has been proposed that the absorption ratio A_{250}/A_{280} is capable of distinguishing between

ps and aps duplexes (25). We measured A_{250}/A_{280} for ps-N7 and aps-N7 as well as for ps-N6 and aps-N6. This parameter decreased with increasing temperature for ps-N7 as well as for ps-N6 (Figure 5), indicating the same ps character of the ps-N7 and ps-N6 duplexes. In contrast, A_{250}/A_{280} increased with temperature for both aps-N7 and aps-N6. We conclude that the intramolecular ps-N7 hairpin formed at low concentration but that some indeterminate intermolecular structure prevailed at the higher concentration used in the FTIR measurements. The T_m of ps-N7 was 20 °C lower than that of the ps-N6 hairpin duplex, in agreement with the destabilizing effect from scattering the guanines in the sequence.

Hypoxanthine Substitution. As a means for establishing the number and identity of guanine nitrogen atoms involved in H-bonding in the ps-hairpin duplexes, we substituted guanines by hypoxanthine, a base analogue lacking the $\text{N}2\text{H}_2$ group. The latter is involved in the H-bonding scheme of Figure 1f but not that of Figure 1e. Thus, if the amino group was not involved in the secondary structure of the ps duplexes, the substitution of guanine by hypoxanthine should not have perturbed their formation or stability. In contrast, the second H-bond of the model in Figure 1f would be disrupted. The stability and the conformation of the structures formed by the hypoxanthine analogues of ps-N6 and ps-N7, denoted ps-N8 and ps-N9, respectively, were studied by spectroscopic methods. In addition, we examined aps-N8 and aps-N9, the hypoxanthine analogues of aps-N6 and aps-N7.

The hypoxanthine substitution induced a large decrease in hyperchromicity and of the T_m values determined by UV spectroscopy of both ps-N8 and ps-N9 relative to the parent ps-N6 and ps-N7 ($\Delta T = 30$ and 13 °C, respectively; Table 2, bottom). These data clearly indicated that the $\text{N}2\text{H}_2$ group of G was important for the formation of the ps duplexes. Lower T_m values were also found, as expected, for the aps hypoxanthine analogues because the *cis*-Watson-Crick I•C base pair has only two H-bonds instead of the three between G and C (Table 2, bottom). As shown in Figure 5 (bottom), the A_{250}/A_{280} ratio versus temperature indicated the formation of partially or fully paired aps duplexes of ps-N8 and aps-N8 as well as of ps-N9 and aps-N9. However, we note that the T_m values of ps-N8 measured by UV and FTIR

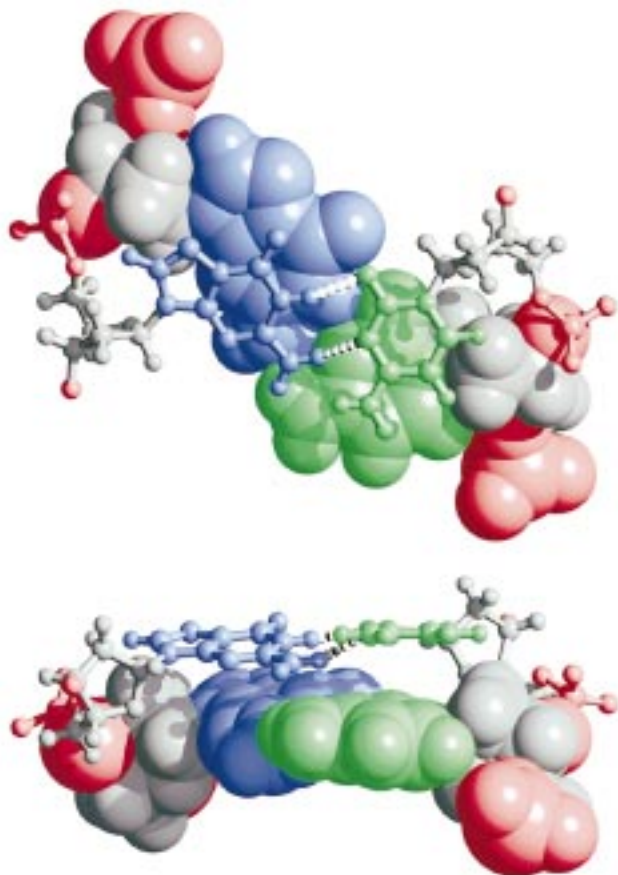


FIGURE 7: Top and side views (top and bottom structure, respectively) of a G•C/C•G dinucleotide in the GGG block of the ps-N1 structure after energy refinement. Color coding: guanine, blue; cytosine, green; sugar, a; phosphate group (including O5' and O3'), red. The H-bonds between G:HN1=C:O2 and G:N1H2=C:N3 are shown as broken white lines. During the energy minimization, the G•C base pair readjusted so as to reduce the clash between the guanine and cytosine amino groups, giving rise to a noticeable propeller twist.

spectroscopy were different, whereas those of aps-N8 were very similar. We conclude that the expected monomolecular structure (a hairpin duplex) formed in the case of aps-N8 but probably not the ps-N8 analogue.

In agreement with the above findings, the FTIR spectra of ps-N8 and ps-N9 also failed to indicate the formation of a ps hairpin duplex (Figure 6). The spectra lacked the characteristic band of the C2=O2 stretching vibration of thymines engaged in *trans*-Watson-Crick pairing at 1683 cm^{-1} . In the case of ps-N8, the 1689 cm^{-1} band (also observed in the aps-N8 spectrum) could be assigned to the H-bonded carbonyl groups of the hypoxanthine residues, but not to free C6=O6 groups. The adenine band was shifted to higher frequencies and its intensity enhanced in ps-N8 as compared to aps-N8, possibly indicating the presence of some unbound adenine residues in the ps-N8 structure at low temperature. The ps-N9 spectrum, even at low temperature, resembled more a melted DNA spectrum than of ps-N8. The relative intensity of the 1689 cm^{-1} band of the associated guanines was decreased, all the carbonyl stretching vibrations were mainly superimposed at 1664 cm^{-1} , and a strong free adenine band was observed at 1627 cm^{-1} .

The various experimental approaches provided consistent evidence for the absence of ps hairpin duplexes with

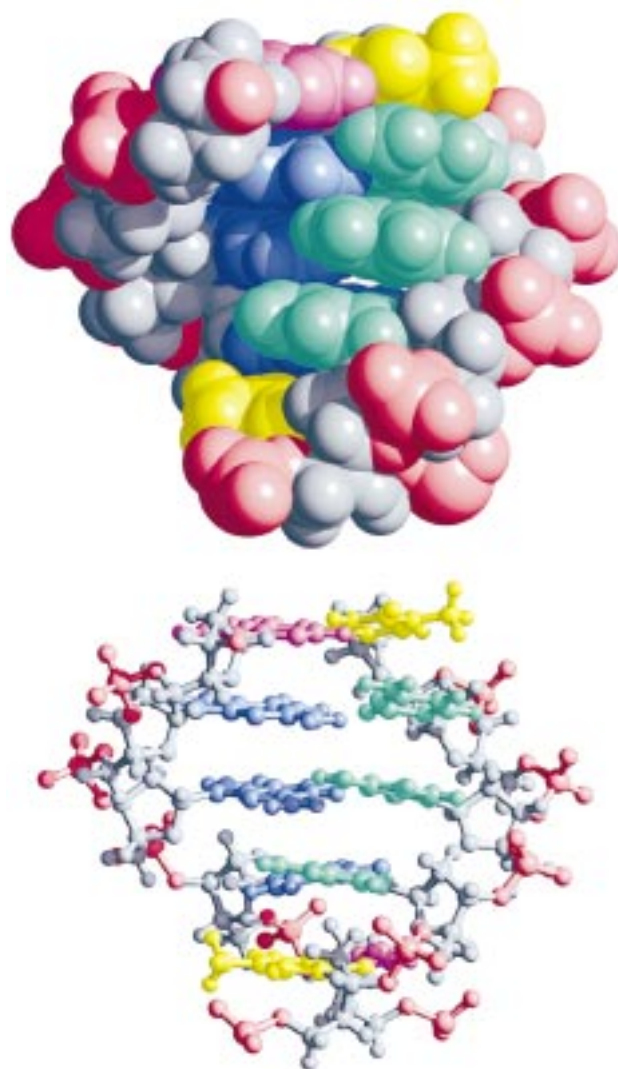


FIGURE 8: Side view of the energy-minimized model of the 5'-AGGGA-3'/5'-TCCCT-3' segment of the ps-N1 molecule. Color coding: guanine, blue; cytosine, green; adenine, magenta; thymine, yellow; sugar backbone, gray; phosphates (including O5' and O3'), red. The propeller twist of the G•C base pairs reduces clash between the N2(G) and the N4(C) amino groups. The bottom view is the same as the top view but as a ball-and-stick model.

hypoxanthine-containing oligonucleotides, whatever the sequence. We conclude that the model with one H-bond (Figure 1e) proposed for sequences with isolated guanines in a previous study (10) did not apply to our molecules, even in the case of ps-N7 (despite the absence of a FTIR spectrum), judging from the effects of the hypoxanthine substitution in ps-N9. All FTIR spectra recorded in the region of base double-bond vibrations were similar for sequences having consecutive or separate guanines (ps-N1, ps-N2, ps-N3, and ps-N6). Thus, up to a content of 40% G•C, we observed that the ps hairpin duplexes either did not form at all or featured G•C base pairs with two H-bonds. Features of this structure (Figure 1f) are further elaborated in the next section.

Model Building and Energy Minimization of the Ps-N1 and Ps-N2 Duplexes. A systematic exploration of start structure parameters (helical twist and rise) was adopted, a minimization strategy intended to explore systematically the energy landscape of DNA conformational states. One can

thereby overcome energy barriers between local minima that cannot be crossed by standard minimization procedures. After energy minimization, the structures with the most favorable energies contained only G•C base pairs with two H-bonds. This finding was independent of the initial H-bonding scheme and the initial sequence (either ps-N1 or ps-N2). The *trans*-Watson–Crick base pairs were similar in all low energy structures, regardless of whether they occurred in blocks as in ps-N1 or were isolated as in ps-N2. The G•C base pairs exhibited a distinct propeller twist, thereby avoiding clash between the N2(G) and N4(C) exocyclic amino groups located on the same side in the *trans*-Watson–Crick G•C configuration (Figure 7). A regular stacking of the G•C base pairs in the ps-N1 structure was found in the low-energy structures (Figure 8). Comparing these results to those from earlier model building of isolated G•C base pairs in ps-DNA structures (10) is not straightforward since the G•C base pairs in the current models were not flanked by homoadenine and/or thymine sequences. The situation of the single G•C base pair described in (10) will be reinvestigated with the multistructure minimization method employed here.

Summarizing Remarks. FTIR and UV spectroscopic measurements have demonstrated that ps hairpin duplexes are formed in sequences containing up to 40% G•C base pairs. We have shown that G•C base pairs are formed. When the guanines are substituted by hypoxanthine, the ps structure is no longer evident, indicating that two H-bonds are required for its stabilization. The existence of propeller twist and a regular stacking of G•C base pairs in the G•C blocks has been proposed by molecular modeling with force field techniques. Scattering the guanines in a mixed sequence leads to a destabilization of the ps duplex. However, this effect is not due to a change in the H-bonding scheme of the G•C base pair.

ACKNOWLEDGMENT

We thank F. Geinguenaud for skillful technical assistance.

REFERENCES

- Pohl, F. M., and Jovin, T. M. (1972) *J. Mol. Biol.* 67, 375–396.
- Wang, A. H.-J., Quigley, G. J., Kolpak, F. J., Crawford, J. L., Van Boom, J. H., Van der Marel, G., and Rich, A. (1979) *Nature* 82, 680–686.
- Ramsing, N. B., and Jovin, T. M. (1988) *Nucleic Acids Res.* 16, 6659–6676.
- Van de Sande, J. H., Ramsing, N. B., Germann, M. W., Elhorst, W., Kalisch, B. W., Kitzing, E. V., Pon, R. T., Clegg, R. C., and Jovin, T. M. (1988) *Science* 241, 551–557.
- Rippe, K., Ramsing, N. B., and Jovin, T. M. (1989) *Biochemistry* 28, 9536–9541.
- Shchylolkina, A. K., Lysov, Yu. P., Il'icheva, I. L., Chernyi, A. A., Golova, Yu. B., Chernov, B. K., Gottikh, B. P., and Florentiev, V. L. (1989) *FEBS Lett.* 244, 39–42.
- Otto, C., Thomas, G. A., Rippe, K., Jovin, T. M., and Peticolas, W. L. (1991) *Biochemistry* 30, 3062–3069.
- Fritzsche, H., Akhebat, A., Taillandier, E., Rippe, K., and Jovin, T. M. (1993) *Nucleic Acids Res.* 21, 5058–5091.
- Pattabiraman, N. (1986) *Biopolymers* 25, 1603–1606.
- Rippe, K., Ramsing, N. B., Klement, R., and Jovin, T. M. (1990) *J. Biomol. Struct. Dyn.* 7, 1199–1209.
- Rippe, K., Kuryavii, V. V., Westhof, E., and Jovin, T. M. (1992) in *Structural Tools for the analysis of protein–nucleic acids complexes. Advances in Life Sciences* (Lilley, D. M. J., Heumann, M., and Such, D., Eds.) pp 81–107, Birkhäuser Verlag, Basel.
- Liu, C. Q., Shi, X. F., Bai, C. L., Zhao, J., and Wang, Y. (1997) *J. Theor. Biol.* 184, 319–325.
- Borisova, O. F., Shchylolkina, A. K., Chernov, B. K., and Tchurikov, N. A. (1993) *FEBS Lett.* 322, 304–306.
- Shchylolkina, A. K., Borisova, O. F., Chernov, B. K., and Tchurikov, N. A. (1994) *J. Biomol. Struct. Dyn.* 11, 1237–1249.
- Tung, C. S., and Carter, E. S. (1994) *CABIOS* 10, 427–433.
- Case, D. A., Pearlman, D. A., Caldwell, J. W., Cheatham, T. E., III, Ross, W. S., Simmerling, C. L., Darden, T. A., Merz, K. M., Stanton, R. V., Cheng, A. L., Vincent, J. J., Crowley, M., Ferguson, D. M., Radmer, R. J., Seibel, G. L., Singh, U. C., Weiner, P. K., and Kollman, P. A. (1997) AMBER5, University of California, San Francisco.
- Tsuboi, M., Takahashi, S., and Harada, I. (1973) in *Physicochemical Properties of Nucleic Acids* (Duchesne, G., Ed.) Vol. 2, pp 91–145, Academic Press, London.
- Liquier, J., Akhebat, A., Taillandier, E., Ceolin, F., Huynh-Dinh, T., and Igolen, J. (1991) *Spectrochim. Acta* 47A, 177–186.
- Sponer, J., and Hobza, P. (1994) *J. Biomol. Struct. Dyn.* 12, 671–680.
- Liquier, J., and Taillandier E. (1996) in *Infrared spectroscopy of Biomolecules* (Mantsch, H. H., and Chapman, D., Eds.) pp 131–158, Wiley-Liss, New York.
- Dagneaux, C., Liquier, J., and Taillandier, E. (1995) *Biochemistry* 34, 14815–14818.
- Dagneaux, C., Gousset, H., Shchylolkina, A. K., Ouali, M., Letellier, R., Liquier, J., Florentiev, V. L., and Taillandier, E. (1996) *Nucleic Acids Res.* 24, 4506–4512.
- Miles, H. T., and Frazier, J. (1972) *Biochem. Biophys. Res. Commun.* 49, 199–204.
- Majoubé, M. (1984) *J. Chim. Phys.* 81, 303–315.
- Jovin, T. M., Rippe, K., Ramsing, N. B., Klement, R., Elhorst, W., and Vojtiskova, M. (1990) in *Structure and Methods* (Sarma R. H., and Sarma M. H., Eds.) Vol. 3, pp 155–174, Adenine Press, New York.

BI981143P